Research Square

Preprints are preliminary reports that have not undergone peer review.
They should not be considered conclusive, used to inform clinical practice,
or referenced by the media as validated information.

Evolution Analysis of Global Polysilicon Trade Patterns and Node Resilience Considering Comprehensive Trade Distance

Jiayan Zeng
Central South University of Forestry and Technology https://orcid.org/0009-0007-2504-8210
Xiangyu Huang
xyhuang@csuft.edu.cn

Central South University of Forestry and Technology https://orcid.org/0009-0002-1245-5611
Liuguo Shao
shaoliuguo@csu.edu.cn

Central South University, Business School https://orcid.org/0000-0002-2976-5037
Zhongwei Wang
Central South University of Forestry and Technology
Yihua Li
Central South University of Forestry and Technology https://orcid.org/0000-0002-3228-2562

Research Article

Keywords: Polysilicon Trade, Weighted Directed Complex Network, Geopolitical Relationship Index, Comprehensive Trade Distance, Node Resilience

Posted Date: May 11th, 2026

DOI: https://doi.org/10.21203/rs.3.rs-9632573/v1

License: This work is licensed under a Creative Commons Attribution 4.0 International License.
Read Full License

Additional Declarations: The authors declare no competing interests.

Article

Evolution Analysis of Global Polysilicon Trade Patterns and Node Resilience Considering Comprehensive Trade Distance

Jiayan Zeng [a,b], Xiangyu Huang [a,c,*], Liuguo Shao [d,e,*], Zhongwei Wang [a,c], Yihua Li [a,c]

a Central South University of Forestry and Technology, School of Economics and Management, Changsha 410004, China;
b Ocean University of China, School of Economics, Qingdao 266100, China;
c Hunan Key Laboratory of Intelligent Logistics Technology, Changsha 410004, China;
d Central South University, Business School, Changsha 410083, China;
e Central South University, Institute of Metal Resources Strategy, Changsha 410083, China;
* Correspondence: xyhuang@csuft.edu.cn (X. Huang), shaoliuguo@csu.edu.cn (L. Shao)

Abstract: Against the backdrop of the global clean energy transition, polysilicon—as the core feedstock for photovoltaics—occupies a critical nexus in energy security and technological sovereignty. To overcome limitations of unidimensional edge weight specifications in extant network models, this study integrates trade data and GDELT geopolitical event data from 2004–2023, constructing a "comprehensive trade distance" weighted network model fusing trade intensity, export competition strength, and geopolitical relationships. This framework systematically quantifies multidimensional impedance to trade pathways and simulates node resilience evolution under alternative disruption scenarios. The findings indicate that global polysilicon trade exhibits three-phase characteristics—steady growth, rapid expansion, and oscillatory decline—while the network structure demonstrates "breadth extension, depth concentration" evolution. Crucially, node resilience is fundamentally determined by the "evolutionary corridor" formed by the network topology, while geopolitical linkages act as differential modulators. Geopolitical risk does not function as a uniform external pressure but as a node-specific filter that exerts asymmetric correction and perturbation on individual resilience trajectories through bilateral linkages. Supply concentration and geopolitical risk jointly shape the vulnerability distributions among core importers. This study furnishes scientific foundations for supply chain risk quantification and resilience governance in strategic raw material supply chains.

Keywords: Polysilicon Trade; Weighted Directed Complex Network; Geopolitical Relationship Index; Comprehensive Trade Distance; Node Resilience

1. Introduction

Amidst converging consensus that photovoltaic (PV) deployment constitutes a core pathway toward carbon neutrality [1], polysilicon—as an irreplaceable feedstock—occupies a critical nexus where supply security directly implicates national energy transition and technological sovereignty [2]. The strategic significance of polysilicon manifests in both industrial scale—China's PV installations surged 148.12% year-on-year in 2023—and production technology, where cold hydrogenation processes achieve 90% energy reduction, determining sustainable development capacity. Intensifying great-power competition has rendered international trade susceptible to geopolitical influences, with "friend-shoring" trends becoming pronounced [3]. The interplay between geographic concentration and geopolitical barriers amplifies supply chain complexity and disruption risks [4]. Although extant research has illuminated physical trade flows and topological vulnerability [5], measurement approaches remain predominantly confined to unidimensional trade volume metrics, failing to embed export competition and geopolitical affinity within network weights—thereby proving insufficient for reflecting compound resistance under "friend-shoring" trends. To surmount this, constructing multidimensional weighted trade networks integrating

trade scale, competition intensity, and geopolitical affinity is necessitated to accurately capture supply chain flow resistance and identify critical hubs.

Extant research indicates that the Global Polysilicon Trade Network (GPSTN) has exhibited increasingly complex evolutionary characteristics since 2000 [6]. Contemporary studies predominantly employ complex network theory and UN Comtrade statistics to dissect topological structure and critical nodes [7]. Analysis of the Polysilicon Trade Dependency Network (PSTDN) has revealed trade community delineations during 1995–2019 [2]. Notably, the polysilicon supply chain is deeply embedded within geopolitical configurations, with institutional factors including trade policy constituting imminent threats. For instance, geographic concentration renders linkages like China–Vietnam and Southeast Asia–North America susceptible to disruption from geopolitical friction [5]. Such risks underscore the imperative of incorporating geopolitical dimensions into trade network weights. Accordingly, scholars have constructed multidimensional analytical frameworks for supply risk, quantifying national vulnerability under disruption scenarios [8].

Broader scholarship has achieved progress in quantifying geopolitical dimensions using the GDELT database, which monitors global news across 100 languages to identify critical events and entities [9]. Methodologically, studies have integrated GDELT big data with complex network techniques to enhance precision. Sada et al. [10] constructed Asian political distance networks, revealing diplomatic centrality through international cooperation analysis. Yao et al. [11] employed GDELT data to analyze COVID-19 assistance events, demonstrating the implications of international aid for global crises. Guo et al. [12] developed cross-border cooperation networks to examine interactions amid geopolitical tensions, while Liu et al. (2023) focused on risk perception analysis, emphasizing GDELT's source breadth and temporal granularity. Regarding indicator construction, Mo et al. [13] validated GDELT's capacity for capturing shifts in international relations, and Wang et al. [14] found that geopolitical threats impede green technology development, while also affecting energy transition trajectories through channels like trade openness.

These studies demonstrate that geopolitical factors can be embedded within networks through event data. However, characterizations of geopolitical dimensions have often relied upon qualitative or simplistic quantitative methods, exhibiting limited capacity for effective translation into network analysis weights. Regarding resilience, the concept denotes the capacity of systems to restore functions following stress [15]. Definitions vary across disciplines, encompassing ecological, engineering, adaptive, and economic resilience [16-21]. In trade network research, resilience manifests as the capacity to reconfigure structure and adapt to new equilibria under perturbation [22]. Essentially, resilience reflects the survival logic of systems within multidimensional dynamic processes [23].

In complex network research, indicators like betweenness and PageRank centrality measure node importance[24-27]. Dynamic resilience denotes the capacity to maintain performance through structural adjustments [28]. Recent scholarship has identified core countries as determinative for network resilience in crude oil, grain, and energy trade [29-31]. Yu et al.[32] noted that elevated trade concentration renders iron ore networks susceptible to shocks, advocating for supply chain diversification. Shen et al. [33] found that bottleneck nodes exhibit particular vulnerability during emergencies. Crucially, Lan and Shao [34] integrated "geopolitical collaboration capacity" into comprehensive assessments of supply chain resilience. Furthermore, Wu et al. [35] found that PV networks exhibit stronger upward dynamic trends than traditional energy, while Wang and Chen [36] pointed out varying shock resistance across wind power industrial chains. Additionally, Wei et al.[37] validated functional recovery under dynamic shocks through an extreme event simulation model for oil trade networks. Nevertheless, these studies uniformly omit geopolitical factors from in-depth resilience analysis, constituting a significant lacuna.

Trade network weighting constitutes a core procedure for revealing dependency relationships. Zhao et al. [38] and Zhang et al. [39] employed trade values as direct weights for wind turbines and gallium, establishing a mature paradigm centered on trade volume [40-43]. However,

resource supply chains are profoundly shaped by macro-environmental policies and co-production mechanisms. Shao et al. [44] demonstrate that under co-production regimes, market interdependencies and carbon constraints exert determinative influences on gallium supply. Such mechanisms indicate that unidimensional weighting is insufficient for capturing the multiple attributes of trade pathways, necessitating edge weight construction integrating economic and political indicators.

In summary, to address the failure of unidimensional trade network analyses in capturing geopolitical risks, this study makes two theoretical contributions. First, we construct a geopolitical relationship quantification model that enhances indicator differentiation via subjective-objective weighting, robust statistics, and power transformations. Second, we propose a "comprehensive trade distance" framework integrating economic, geopolitical, and competitive dynamics to reflect authentic dependency structures. Applying this to the global polysilicon trade network, we reveal evolutionary mechanisms of trade patterns and assess both node resilience and network vulnerability through multi-scenario simulations.

The remainder of this paper is organized as follows: Section 2 presents data and model construction; Section 3 analyzes simulation results; Section 4 concludes.

2. Data Sources and Research methodology

2.1. Data source and Research Framework

2.1.1. Trade data source

This study examines polysilicon (HS 280461, silicon purity ≥ 99.99%) as the research object [38], drawing upon UN Comtrade data to obtain trade records for 210 countries and territories from 2004–2023, encompassing approximately 11,000 import and 9,000 export observations. To ensure data consistency and analytical reliability, we employ import data as primary and export data as supplementary for imputation, incorporating Hong Kong and Macau into China statistics. Concurrently, to exclude disturbances from prices and exchange rates, physical trade volume serves as the core indicator. For missing trade volume observations, we apply stratified mean imputation: after grouping by HS code and year, missing values for top-ten importers within each group are filled using non-missing means from their respective top-ten peers; remaining missing values are replaced by arithmetic means of all non-missing records within the group, thereby preserving data structure consistency and representativeness.

2.1.2. Geopolitical data source

Geopolitical data for this study are sourced from the GDELT event database, which relies upon real-time monitoring of global news media to extract structured event information with 15-minute updates[45]. GDELT employs the Goldstein scale to quantify each event, with scores ranging from –10 to 10: positive values denote cooperative impacts, negative values indicate conflictual impacts, and absolute magnitudes represent event intensity [46, 47]. From approximately 730 million raw records, we filter approximately 140 million valid observations of interstate news events, furnishing a high-quality structured foundation for constructing **geopolitical distance** indicators.

2.1.3. Research Framework

This study integrates UN Comtrade and GDELT databases to generate **trade volume** metrics and quantified **geopolitical relationship** indicators, respectively. Through CRITIC-expert hybrid weighting, we fuse three dimensions—**trade intensity**, export competition, and **geopolitical distance**—to construct a **dual-weighted global polysilicon weighted directed complex network model**. Subsequently, we analyze **efficiency**, **centrality**, and multi-scenario shock resistance across three dimensions: **trade patterns**, **node influence**, and **resilience**. This yields policy implications for strategic **supply chain risk** identification and **geopolitical governance resilience** enhancement, as illustrated in **Fig. 1**.

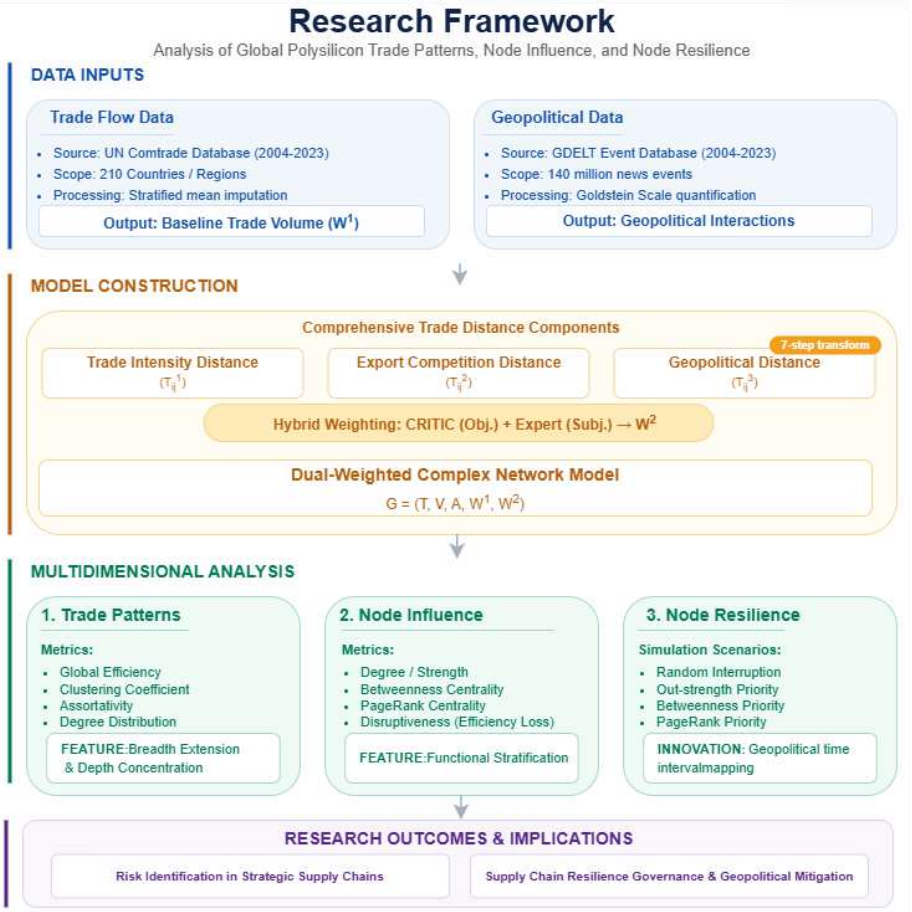


Fig. 1. Research framework flowchart.

2.2. Graph theory model construction and evaluation indicators

2.2.1. Model construction

This study conceptualizes countries or territories participating in polysilicon trade as nodes and their trade relationships as edges, constructing a complex network model for polysilicon trade characterized by a dual-weight structure with trade volume and comprehensive trade distance as edge weights. This network can be formalized as:

$$G = (T, V, A, W^1, W^2) \quad (1)$$

where T in Eq.(1) denotes the study year; G represents the global polysilicon trade network in year T; V is the node set comprising all countries or territories participating in polysilicon trade during that year; adjacency matrix A indicates whether trade relationships exist between node pairs; W^1 is the trade volume weight matrix reflecting actual trade scale; and W^2 is the comprehensive trade distance weight matrix, whose construction constitutes a core contribution of this study. By integrating three dimensions—trade intensity, export competition strength, and geopolitical relationships—W^2 systematically characterizes flow resistance and stability within trade networks, effectively substituting traditional physical distance-based weighting systems and furnishing a more realistic theoretical and computational framework for strategic raw material trade network analysis.

2.2.2. Comprehensive trade distance model combining subjective and objective weighting

Based on the framework outlined above, this section elaborates on the construction method of the comprehensive trade distance weight. To overcome the limitations of single indicators or subjective weighting, this study adopts a strategy combining subjective and objective weighting

to scientifically integrate and assign weights to three dimensions: trade proximity, export competition intensity, and geopolitical relations.

(1) Trade Intensity Distance

We introduce **trade intensity distance** T_{ij}^{1}, transforming raw **trade flows** into economically meaningful distance metrics [41]. Through logarithmic compression and inverse mapping, we achieve conversion from high **trade volume** to low distance, with the specific formulation:

$$T_{ij}^{1} = 1 + \ln\mathrm{Max}\left(w_{ij}^{1}\right) - \ln\left(w_{ij}^{1}\right) \quad (2)$$

Where in Eq.(2) T_{ij}^{1} denotes trade intensity distance between nodes V_i and V_j; $\mathrm{Max}\left(w_{ij}^{1}\right)$ represents the maximum edge trade volume in the network; and w_{ij}^{1} indicates trade volume between nodes V_i and V_j.

(2) Export Competition Intensity Distance

Export competition intensity distance T_{ij}^{2} measures potential competitive relationships and implicit risks between countries or territories in polysilicon export markets. Building upon extant research [48], we define export competition intensity C_{ij} as:

$$C_{ij} = \frac{w_i^{out} + w_j^{out}}{\sum_{k=1}^{N} w_k^{out}} \times \left\{1 - \frac{\left|w_i^{out} - w_j^{out}\right|}{w_i^{out} + w_j^{out}}\right\} \quad (3)$$

where in Eq.(3) $w_i^{\mathrm{out}}, w_j^{\mathrm{out}}$, and w_k^{out} denote out-strength of nodes V_i, V_j, and global polysilicon outstrength, respectively; N represents total network node count. Higher C_{ij} values indicate closer export scale proximity and intensified competition. To address nodes with zero export values, we apply Laplace smoothing by replacing zeros with the minimum positive value of 1, ensuring computational stability. Competition intensity is subsequently transformed into competition distance through logarithmic transformation (see Eq.(4)):

$$T_{ij}^{2} = 1 + \ln\left(C_{ij}\right) - \ln\mathrm{Min}\left(C_{ij}\right) \quad (4)$$

This transformation reinforces the intuitive interpretation that greater competition intensity corresponds to increased distance, accentuating competitive differentials across node pairs

(3) Geopolitical Relationship Distance

Geopolitical relationship distance T_{ij}^{3} quantifies political relationship proximity between nodes, with higher values indicating tighter relationships and correspondingly shorter distances. This indicator draws upon the GDELT database, measuring bilateral news event counts and Goldstein interaction intensities [49], with the computational procedure illustrated in **Fig. 2**. The methodology comprises: first, calculating annual geopolitical relationship indices $\left(R_{ij}^{t}\right)_t$ between nodes; second, computing mean $\bar{R}_{ij}$ and median $\check{R}_{ij}$ across the study period, with their arithmetio average serving as the base relationship score R_{ij}; third, applying power transformation to optimize distributional properties and enhance differentiation—given low density in the first and ninety-ninth percentiles, winsorization at these thresholds mitigates extreme value effects; fourth, imputing missing values using mean substitution; and finally, deriving geopolitical relationship distance T_{ij}^{3} through logarithmic transformation

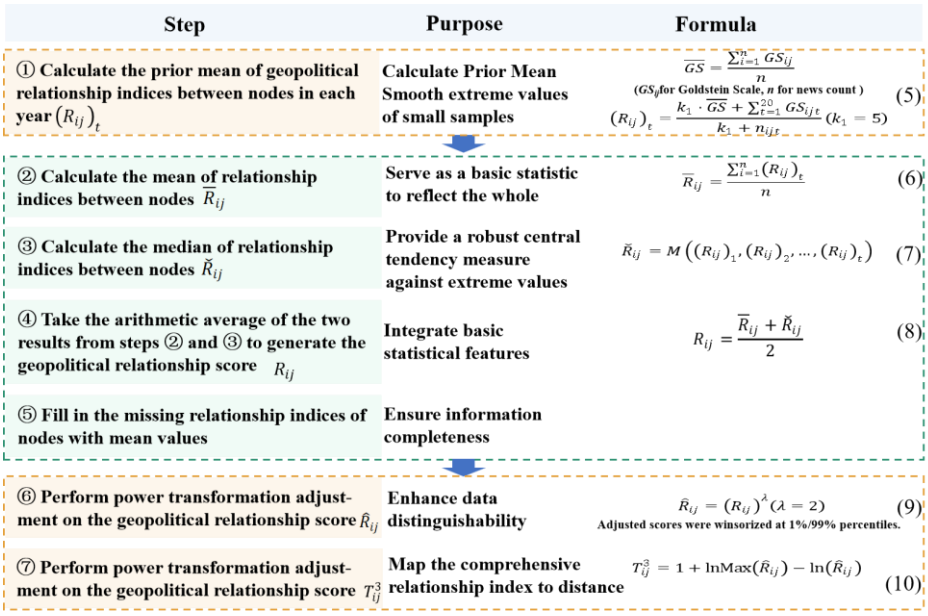


Fig. 2. Measurement Model for Geopolitical Relationship Distance.

(4) Comprehensive Trade Distance

Comprehensive trade distance w_{ij}^2 is constructed through integration of the aforementioned three indicators. **Polysilicon supply chain** stability is profoundly constrained by economic supply-demand dynamics, market competition, and **geopolitical** environments. Unifying these three heterogeneous dimensions into **network** "**distance**" enables systematic quantification of comprehensive risk resistance along **trade pathways**. This fused indicator transcends the scale-obscuring effects of unidimensional **trade volume weights**, precisely illuminating "**latent vulnerabilities**" within **networks**—effectively identifying vulnerable dependency paths characterized by substantial **trade volumes** yet elevated **geopolitical risks** and high **disruption** susceptibility. Such reconstruction rectifies overestimation of **node security** in extant models, furnishing a scientific **edge weight** foundation for multi-scenario **resilience** assessment. To scientifically determine dimensional weights, we employ an integrated weighting approach combining CRITIC objective weighting with expert scoring subjective weighting [50]. The specific procedure is illustrated in **Fig. 3**. The methodology comprises: first, standardizing the three distance indicators through unified dimensionless processing Z_{ij}^l, where l indexes the respective distance indicators; second, computing standard deviations δ^l for each indicator and Pearson correlation coefficients r^{lh} between indicators, subsequently calculating information content s^l based on indicator variability and correlation, and deriving objective weights $(\alpha^l)'$ accordingly; concurrently, determining subjective weights $(\alpha^l)''$ through expert scoring; third, obtaining integrated weights α^l through weighted averaging of subjective and objective weights; and finally, synthesizing comprehensive trade distance w_{ij}^2 by aggregating the three distance indicators according to these weights. This approach accommodates both statistical properties inherent in the data and domain knowledge, thereby achieving scientific integration of multidimensional information.

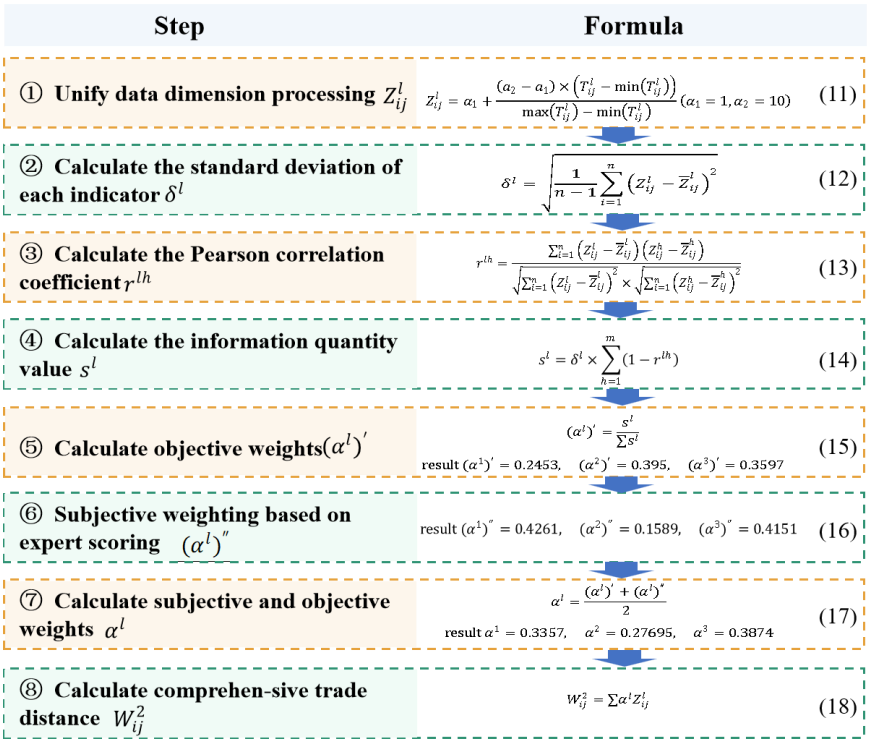


Fig. 3. A Hybrid Weighting Framework for the Comprehensive Trade Distance Model.

2.2.3. Relevant indicators

To systematically examine the overall trade pattern of the global polysilicon trade network, we draw upon analytical dimensions proposed in our prior research, examining transitivity, clustering, hierarchy, and assortativity through computation of unweighted and weighted global efficiency, clustering coefficients, assortativity coefficients, and degree distributions to characterize aggregate network structural properties [41].

To thoroughly assess node roles and functions, we analyze node influence from multiple dimensions. First, following our previous work, we employ out-degree/in-degree and corresponding strength measures, unweighted and weighted betweenness centrality, and PageRank centrality to evaluate node influence and hub status[41, 51]. Second, building upon another prior study, we measure node disruptiveness through global efficiency loss rates and largest connected component total strength loss rates following node removal[52].

Node resilience is quantified as the area under the curve of performance retention rate over time during sustained disruption, representing the cumulative performance level actually maintained by the node during that period. The computational procedure is detailed below.

Supply disruptions in the network occur at discrete time points. To simplify analysis, we assume constant disruption intervals Δt between consecutive disruptions when calculating target node resilience. Different disruption sequences correspond to distinct node removal sequences. The disruption sequence is defined as:

$$\sigma_i = (\delta_1, \quad \delta_2, \quad \cdots \delta_j \cdots \delta_n) \tag{19}$$

Where in Eq.(19) σ_i denotes the sequential disruption supply point sequence; δ_j represents the j-th disrupted supply point; and n indicates total disrupted supply points. This yields the performance retention value sequence for the target node:

$$\left(P_{i,\delta_1}^l, \ P_{i,\delta_2}^l, \ \cdots, \ P_{i,\delta_j}^l, \ \cdots, \ P_{i,\delta_n}^l\right) \tag{20}$$

where in Eq.(20) P_{i,δ_j}^t denotes performance retention value of node V_i following disruption of the j-th supply point δ_j. The performance retention rate sequence is subsequently derived as:

$$R_{i,\delta_j}^l = \frac{P_{i,\delta_j}^l}{P_i^l} \tag{21}$$

$$\left(R_{i,\delta_1}^l,\ R_{i,\delta_2}^l,\ \cdots,\ R_{i,\delta_j}^l,\ \cdots,\ R_{i,\delta_n}^l\right) \tag{22}$$

In Eqs. (21) and (22), R_{i,δ_j}^t represents performance retention rate of node V_i following disruption of supply point δ_j, calculated as the ratio of performance retention value P_{i,δ_j}^t to initial performance value P_i^t.

Let t_{δ_0} denote the disruption initiation time point and t_{δ_n} indicate the disruption time point for node δ_n. Given uncertainty in performance retention rate curves, we apply linear approximation between $t_{\delta_{j-1}}$ and t_{δ_j} for computational simplification. The cumulative performance retention rate during this interval is represented by the trapezoidal area under the curve:

$$\int_{t_{\delta_{j-1}}}^{t_{\delta_j}} R_i^l(t)dt = \frac{\left(R_{i,\delta_{j-1}}^l + R_{i,\delta_j}^l\right) * \Delta t}{2} \tag{23}$$

where in Eq.(23) $\int_{t_{\delta_{j-1}}}^{t_{\delta_j}} R_i^t(t)dt$ denotes the integrated performance retention rate area between disruption of node δ_{j-1} and disruption of δ_j.

To ensure comparability of node resilience across years and nodes, we employ standardized disruption scale settings, uniformly specifying baseline disruption count k across simulations. This enables horizontal comparison under equivalent disruption scales, ensuring fairness and comparability of node resilience measures. The node resilience formula following progressive disruption of k supply points is:

$$\begin{aligned} R_i^l = \int_{t_{s_0}}^{t_{s_k}} R_i^l(t)dt &= \frac{\left(R_{t,\delta_0}^l + R_{t,\delta_1}^l\right)*\Delta t}{2} + \frac{\left(R_{t,\delta_1}^l + R_{t,\delta_2}^l\right)*\Delta t}{2} \\ &\quad + \cdots + \frac{\left(R_{t,\delta_{k-1}}^l + R_{t,\delta_k}^l\right)*\Delta t}{2} \\ &= \sum_{j=1}^{k} \left(\frac{R_{t,\delta_{j-1}}^l + R_{t,\delta_j}^l}{2}\right) * \Delta t \end{aligned} \tag{24}$$

Given that initial performance retention rate equals unity, Eq.(24) simplifies to Eq.(25):

$$R_i^l = \left[\frac{1}{2} + \frac{1}{2}R_{i,\delta_k}^l + \sum_{j=1}^{k-1} R_{i,\delta_j}^l\right] * \Delta t \tag{25}$$

Node resilience is subsequently normalized by dividing by the initial retention value k:

$$\bar{R}_i^l = \frac{R_{i,resistance}^l}{k} \tag{26}$$

Where in Eq.(26) $\bar{R}_i^l$ denotes node resilience of node V_i normalized by P^l performance.

The baseline node resilience model established above characterizes node performance responses under idealized perturbation sequences based on homogeneous assumptions of constant disruption intervals. However, differential geopolitical relationships in reality significantly modulate temporal dynamics of perturbation transmission. To capture this effect, we further map the geopolitical relationship index onto heterogeneous temporal parameters between consecutive disruption events Specifically, we assume that relationship indices between nodes and supply points are proportional to disruption intervals: higher index values indicate closer relationships and consequently slower interference propagation. Building upon this, we modify the baseline node resilience integral model by substituting constant step size Δt with variable intervals Δt_{ij} ,thereby constructing a node resilience computational framework embedded within geopolitical contexts. Accordingly, the time interval function is defined as:

$$\Delta t_{i,\ \delta_j} = \frac{T^3_{i\delta_j}}{\overline{T^3}} * \Delta t \quad (27)$$

Where in Eq.(27) $\Delta t_{i,\delta_j}$ denotes the disruption time interval between node i and its supply point δ_j; Δt represents the constant step size; $T^3_{\delta_j i}$ indicates the geopolitical relationship index between nodes; and $\bar{T}^3$ signifies the mean geopolitical relationship index across all nodes. Substituting into Eq.(24) yields the modified node resilience model (see Eq.(28)):

$$R_i^l = \sum_{j=1}^{k} \left(\frac{R^l_{i,\delta_{j-1}} + R^l_{i,\delta_j}}{2} \right) * \Delta t_{i,\delta_j} \quad (28)$$

3. Results and Analysis

3.1. Evolution of Trade Patterns

Fig. 4 illustrates the overall evolutionary trajectory of the **global polysilicon trade network** during 2004–2023. The upper panel presents temporal trends in aggregate **trade value** and **trade volume**; the central bubble chart focuses on 18 core **trading nodes** including Germany, China, and the United States, with red (export) and blue (import) circles dynamically reflecting **trade scale** evolution; the lower panel depicts temporal changes in **node** count and **edge** count, revealing evolution in **network scale** and **connectivity density**.

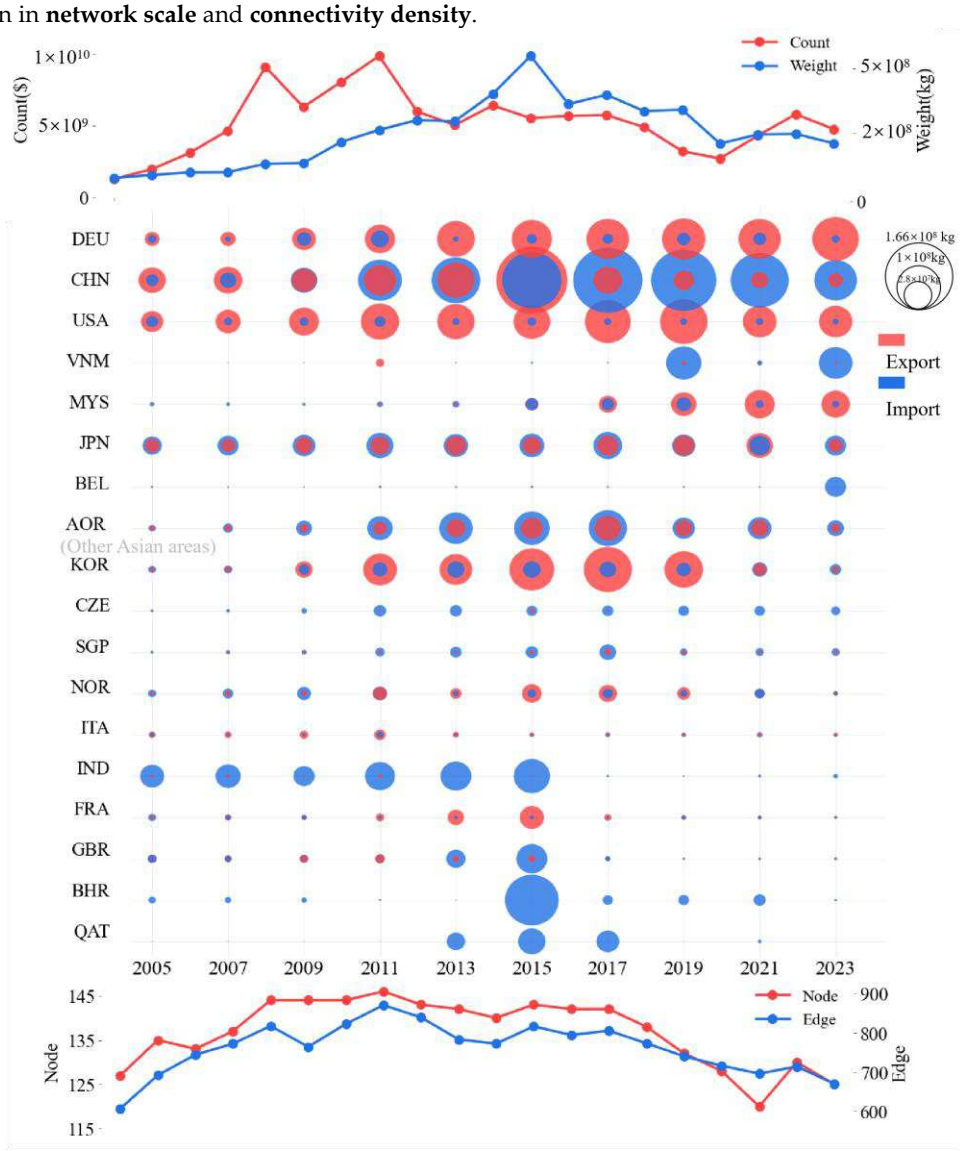


Fig. 4. Bubble chart of global polysilicon trade scale from 2004 to 2023.

The results indicate that **global polysilicon trade volume** expanded from 60,700 to 168,000 tonnes during 2004–2023, representing cumulative growth of approximately 177% with an annual growth rate of 5.2%. This exhibits three-phase fluctuation characteristics—steady growth, rapid expansion, and oscillatory decline—reflecting complex evolutionary processes characterized by concurrent **scale expansion** and **structural adjustment** (**Table 1**). **Node** and **edge** counts in the **trade network** demonstrate corresponding phased synchronous changes.

Table 1. Analysis of Phase-Wise Fluctuation Characteristics in Polysilicon Quartz

Stage	Years	Trend Description
Steady Growth Period	2004–2008	Increased from 60,700 tons to 104,700 tons, representing a growth of 72.4%.
Rapid Explosive Growth Period	2009–2015	Surged sharply from 106,900 tons to 438,400 tons, with an increase of 310.1%.
Fluctuating Decline Period	2016–2023	Fell back from 289,600 tons to 168,100 tons, marking a decrease of 41.9%.

Global polysilicon trade is intimately linked to the photovoltaic industry, with demand fluctuations directly influenced by photovoltaic installation cycles. From the demand perspective, Chinese imports exhibit an inverted-U trajectory, transitioning from rapid ascent to gradual decline, reflecting its transformation from demand-driven growth to enhanced self-sufficiency; Vietnam has rapidly emerged as a novel demand center, becoming a critical node in supply chain regionalization and restructuring. From the supply side, Germany has achieved steady export growth driven by technological advancements, the United States exhibits resource-driven cyclical fluctuations, and Malaysia has experienced exponential growth. In contrast, China's exports have declined significantly from their peak [2, 53], attributable to the domestic absorption of raw materials by its vast downstream manufacturing capacity. Collectively, the global supply chain is accelerating restructuring from a China-centric processing hub toward diversified technological gradients and regionalized systems [54].

The 2008 financial crisis and 2020 COVID-19 pandemic affected polysilicon trade through markedly distinct mechanisms. The 2008 financial crisis induced a 30.8% decline in trade value during 2009, yet trade volume remained essentially stable. This suggests that financial shocks initially impact prices and transactional value, with effects on physical flows manifesting relatively gradually. By contrast, COVID-19 in 2020 simultaneously reduced both trade value and trade volume, generating an "acute shock." This contrast corroborates [55] crisis taxonomy: financial crises permeate trade gradually, whereas public health events inflict immediate disruptions.

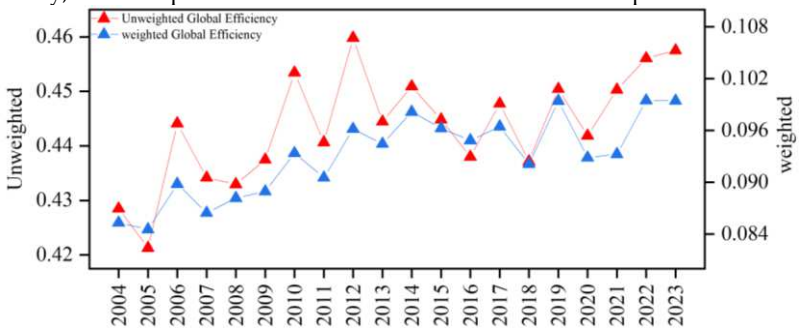


Fig. 5. Evolution of global efficiency of the network from 2004 to 2023.

Fig. 5 reveals that both unweighted and weighted global efficiency of the polysilicon trade network exhibited upward trajectories during 2004–2023, with weighted efficiency increasing by

approximately 16.6%—substantially exceeding the 6.8% growth in unweighted efficiency. This indicates that enhanced network transmission performance derives not merely from topological connectivity optimization, but more critically from comprehensive trade distance reduction attributable to intensified trade relationships and moderated export competition. Network responses to external shocks demonstrate structural differentiation: COVID-19 induced synchronous declines in both efficiency measures, reflecting immediate supply chain disruption impacts; conversely, weighted efficiency rose countercyclically following the financial crisis, potentially attributable to significantly reduced export competition intensity that offset trade volume declines, thereby shortening comprehensive distance and elevating transmission efficiency—highlighting this indicator's pivotal role in modulating network shock resistance.

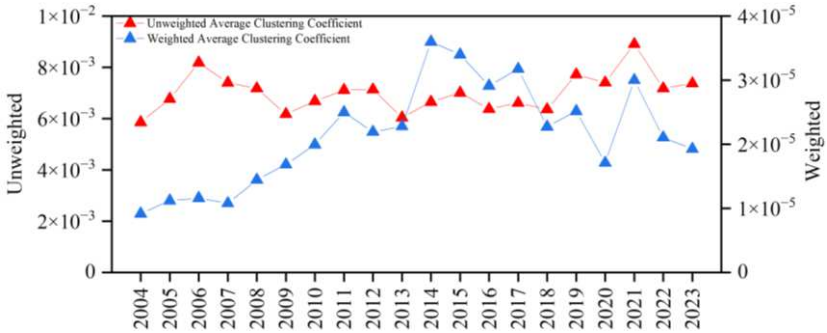


Fig. 6. Evolution of average clustering coefficient of the network from 2004 to 2023.

Fig. 6 indicates that clustering in the global polysilicon trade network has exhibited fluctuating intensification over the past two decades, with weighted average clustering coefficient surging 111%—reflecting supply chain clustering and core-periphery consolidation. The network manifests dual response patterns to external shocks: post-2008 financial crisis, unweighted clustering coefficient declined and connectivity loosened, yet weighted clustering coefficient rose countercyclically as core trade relationships strengthened, displaying pronounced defensive contraction characteristics; by contrast, the 2020 pandemic shock induced synchronous weakening in both connectivity and intensity, with weighted clustering coefficient declining 32.1%—reflecting more direct and comprehensive interference with actual trade flows.

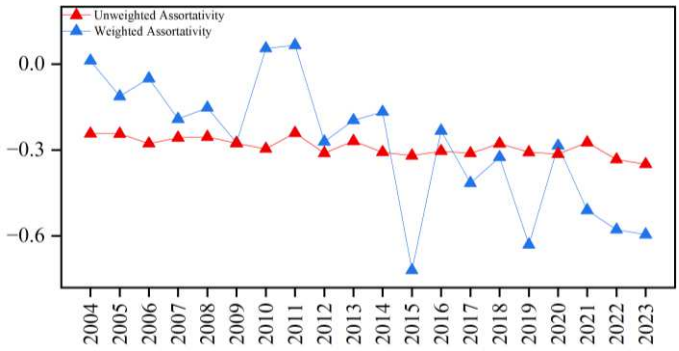


Fig. 7. Evolution of assortative of the network from 2004 to 2023.

The assortativity coefficient of the polysilicon trade network illuminates underlying logic of structural evolution. This coefficient captures node connection preferences based on trade scale: positive values indicate propensity for similar-scale nodes to connect, whereas negative values signify tighter connections between large and small nodes. As **Fig. 7** demonstrates, unweighted assortativity remains persistently negative, indicating stable disassortativity in topological structure with dominant hub positions occupied by few core nodes. Weighted assortativity, however, fluctuated between positive and negative values before 2011, then turned sharply and persistently

negative from 2015 onward—marking fundamental transformation in actual trade flow structure from early "strong-strong" alliance tendencies toward "strong-weak" connection patterns, with trade intensity highly concentrated in core nodes.

This polarization trend has been predominantly shaped by the interplay of macroeconomic fluctuations and industry-specific policies. The 2008 global financial crisis triggered the initial decline. Between 2011 and 2012, anti-dumping and countervailing duty investigations initiated by Europe and the United States erected tariff barriers and disrupted direct trade among major economies, dismantling the core "strong-strong" trade loop. Subsequently, China's suspension of the polysilicon processing trade policy in 2014 and 2015 eliminated a major duty-free channel, redirecting supply routes toward peripheral processing nodes [56]. This shift caused the weighted assortativity coefficient to plummet into negative territory by 2015. Compounded by the COVID-19 pandemic in 2020, this metric has remained highly negative, indicating that successive external shocks have not diversified the network but have instead entrenched a fragile "strong-weak" linkage structure.

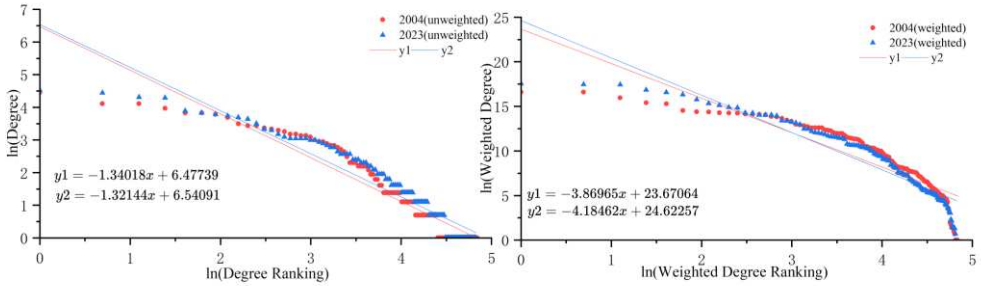


Fig. 8. Evolution of degree distribution of the network in 2003 and 2024.

Fig. 8 presents degree-rank curves for the global polysilicon trade network in 2004 and 2023 under double-logarithmic coordinates. Results indicate that unweighted network slope β declined slightly from 1.34 (2004) to 1.32 (2023), whereas weighted network βw increased from 3.86 to 4.18—signifying diminished hierarchy in unweighted networks yet intensified hierarchy in weighted networks. Although broader country participation renders connectivity distribution more uniform, trade volume further concentrates toward few core nations. The global polysilicon trade network exhibits "breadth extension, depth concentration" evolution: trade linkages broaden while industrial concentration and scale effects enhance core countries' control over trade volume. This characteristic is further corroborated in trade bloc evolution, as illustrated in **Fig. 9** and **Table 2**.

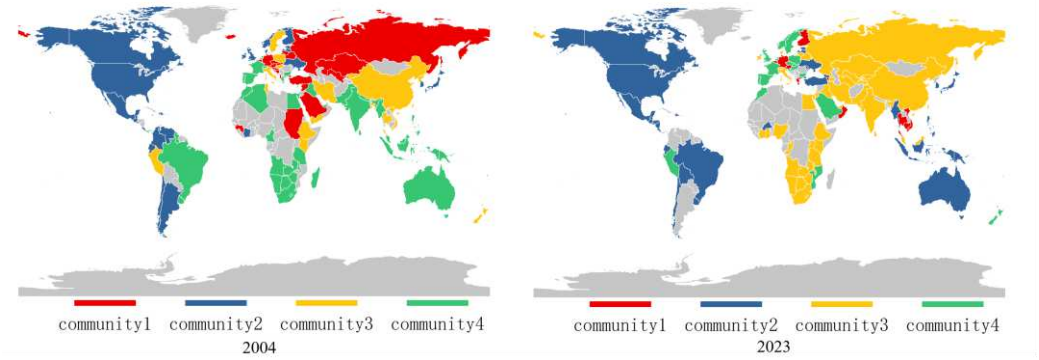


Fig. 9. Distribution of trade groups of the network in 2004 and 2023.

Table 2. Detailed list of major trade group members in 2004 and 2023.

Network Type(2004)	Classification of Trading Blocs	Number	Network Type(2023)	Classification of Trading Blocs	Number
Community1	DEU(85) AUT(15) RUS(10) SVN(3) CZE(3) SAU(2) BEL(2) TUR(0.67) SVK(0.07) UZB(0.0007) etc.	21	Community1	DEU(778) VNM(395) BEL(156) FIN(2) AUT(1) THA(1) etc.	11
Community2	USA(182) JPN(169) GBR(49) KOR(20) NOR(17) UKR(10) CAN(4) MEX(2) DNK(2) FIN(2) etc.	31	Community2	USA(401) JPN(225) KOR(60) SGP(28) TUR(12) GBR(5) AUS(1) IDN(1) CAN(0.3) MEX(0.3) UKR(0.8) PHL(0.4) etc.	37
Community3	CHN(274) ITA(17) NZL(15) POL(2) THA(1) IRN(1) ROU(0.4) VNM(0.05) etc.	20	Community3	CHN(711) MYS(301) RUS(15) ITA(12) DNK(11) IND(8) BHR(2) UZB(2) ZMB(1) ZAF(0.4) ARE(0.08) etc.	52
Community4	IND(200) FRA(13) BHR(13) AUS(12) ESP(8) MYS(7) BRA(6) NLD(4) SGP(3) ARE(1) PHL(1) ZAF(1) IDN(0.96) ZMB(0.05) etc.	50	Community4	CZE(29) SVK(15) NOR(14) NLD(6) FRA(5) ESP(4) ROU(1) POL(0.4) etc.	22

Note: Values in parentheses denote **node total strength**, measured in 10^5kg.

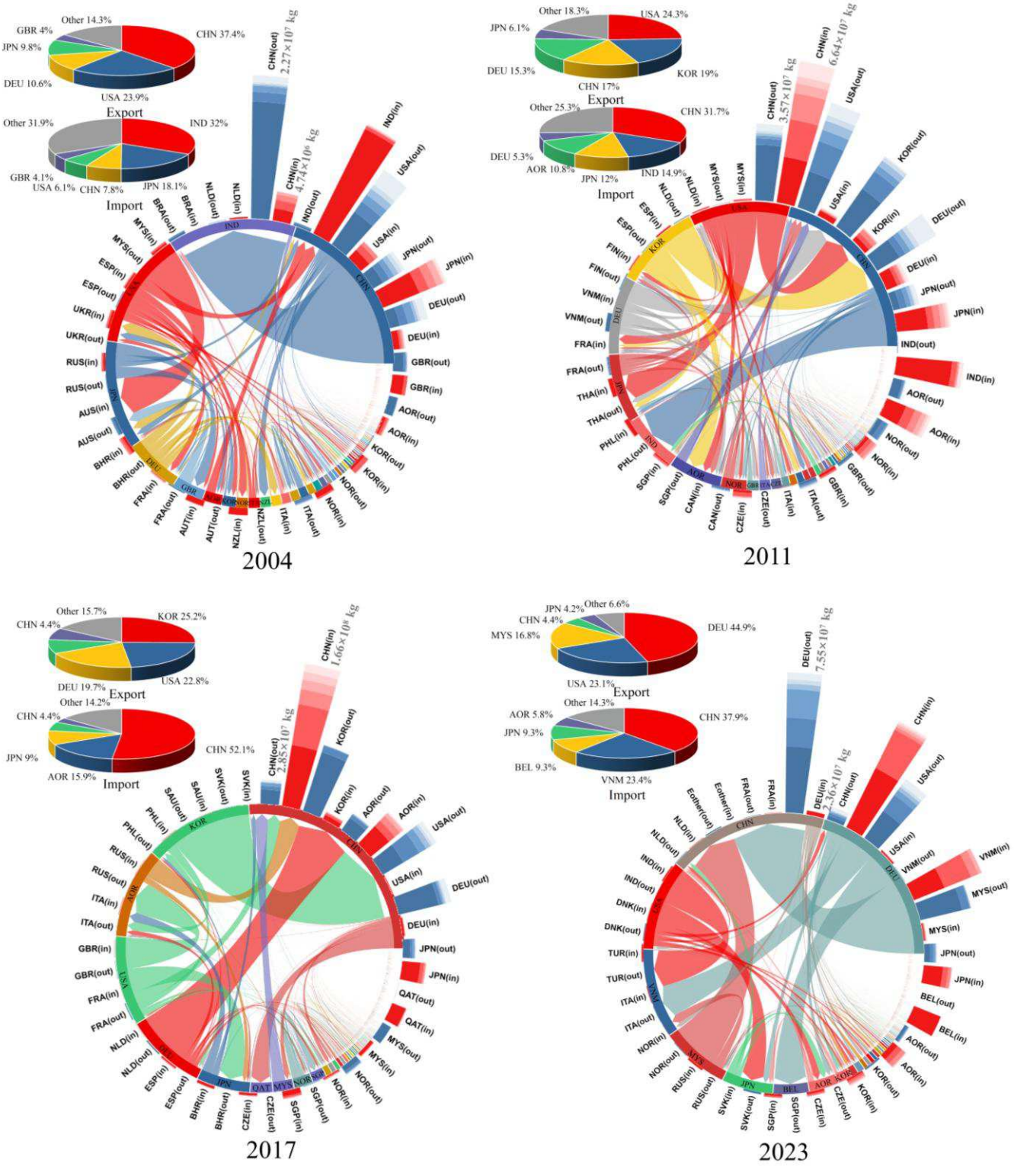
Table 2 demonstrates trade patterns evolving from quadruple equilibrium toward tripolar dominance. German trade volume surged from 85,000 to 778,000 tonnes; China increased from 274,000 to 711,000 tonnes, consolidating its Asian supply chain hub status; and the United States rose from 182,000 to 401,000 tonnes. Conversely, the Indian bloc, formerly trading 200,000 tonnes, completely exited the core network, signifying a high concentration of global trade toward three major centers.

Emerging critical nodes achieved substantial expansion, propelling network regionalization and specialization. The ascent of Asian supply chains is pronounced: Vietnam (395,000 tonnes) became a core pillar of the German bloc, while Malaysia (301,000 tonnes) deeply integrated into China-dominated networks. Simultaneously, intra-European technical collaboration networks formed around the Czech Republic and Slovakia, averaging below 29,000 tonnes and exhibiting refined specialization.

Three key forces drive this profound evolution. First, geoeconomic restructuring propelled trade adjustments; for instance, Russia's shift from the German to the Chinese bloc exemplifies strategic reorientation. Second, the global technological revolution generated novel demand, with explosive growth in semiconductors and photovoltaics furnishing sustained momentum. Third, global industrial chain restructuring facilitated specialized division systems, with processing relocation to Southeast Asia collectively shaping current patterns of regionalization and specialization.

3.2. Evolution of core node influence

To analyze **node influence** and its evolution within **trade networks**, we visualize four critical years—2004, 2011, 2017, and 2023—through topological diagrams. Each diagram employs a dual-layer structure: inner chord diagrams depict **trade volume** and flow directions between **nodes**; outer circular bar charts illustrate influential **nodes** and their top-five **trading partners**' import and export compositions, simultaneously revealing **node trade volume** shares and **trade dependency** structures.



AOR: Other Asian areas.

Fig. 10. Evolution of network topological structure.

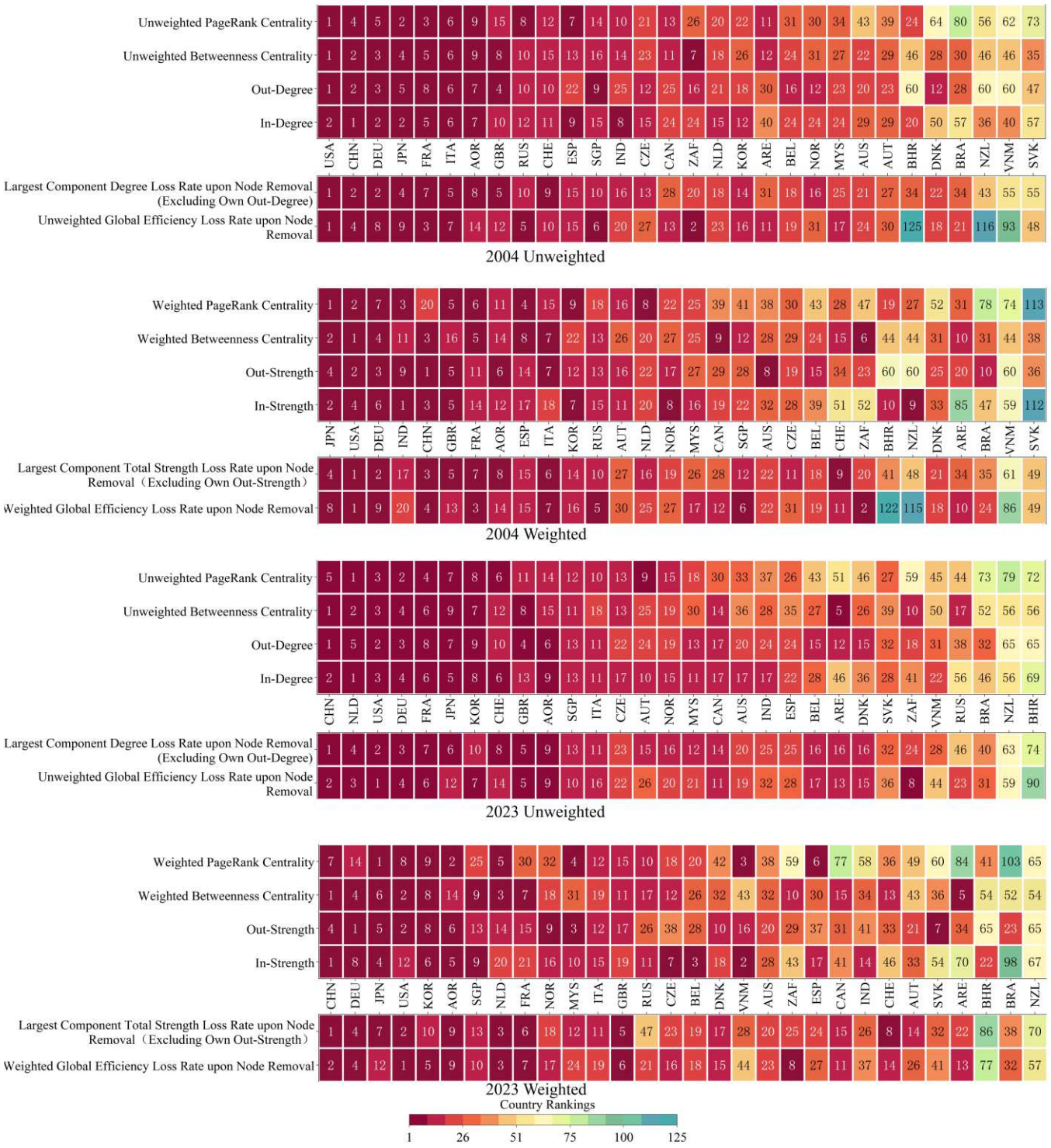
Fig. 10 indicates that the global polysilicon trade network has evolved into a structure characterized by high centralization, efficiency, and risk concentration. The supply side now forms a "dominance triangle": Germany drives high-value exports via technological advantages [57], the United States leverages cost and supply chain strengths [57, 58], and Malaysia serves as a critical

transshipment hub. On the demand side, China has transitioned from a primary supplier into the world's largest demand center, while Vietnam has ascended as the second-largest demand country.

This pronounced geographic concentration induces pathway singularization and profound network vulnerability. Current trade relies on a few primary routes characterized by extreme dependencies, exemplifying by China's reliance on Germany and Vietnam's reliance on Germany and the US. Consequently, localized disruptions propagate rapidly throughout the global supply chain, underscoring the urgent need for diversification and technological innovation.

To systematically assess node influence, we analyzed unweighted and weighted rankings for 2004 and 2023, with detailed results presented in **Fig. 11**. The analysis utilized key centrality indicators, including degree, betweenness, and PageRank, along with simulated removal loss rates. Results indicate that network power has bifurcated into two distinct strata: a "structural control layer" governing connectivity and intermediary functions, exemplified by China and the Netherlands, and a "flow dominance layer" controlling high-intensity trade, consisting of Germany, Japan, and the US. Over this period, Southeast Asian nations ascended rapidly in trade scale, while India's demand position eroded.

Ultimately, network dominance has shifted from pure topological connectivity to a dual reliance on structural and flow advantages. The network exhibits a "dispersed form yet concentrated essence"—while superficial connections have diversified, critical resources remain heavily concentrated within a few core nodes, constituting the structural root of its concurrent efficiency and vulnerability.



AOR: Other Asian areas.

Fig. 11. Heatmap of node centrality and disruptiveness rankings in 2004 and 2023.

Fig. 11 reveals a marked disjunction between node influence and node disruptiveness for select nodes: Japan exhibited the highest weighted PageRank in 2023, indicating exceptional trade relationship quality, yet its export disruption generated modest weighted global efficiency loss rates, suggesting high substitutability of its connections. Vietnam displayed extremely high weighted in-strength but ranked low on disruption indicators, reflecting structural constraints in-

herent to its terminal node position. This divergence demonstrates that singular centrality indicators are insufficient for assessing systemic risk; network roles and connection substitutability jointly determine potential shock magnitude.

Overall, centrality indicators correlate positively with network disruptiveness following export disruption, though correlation intensities vary across performance metrics. To further quantify these relationships, we compute Pearson correlation coefficients between indicators, presented in **Fig. 12**.

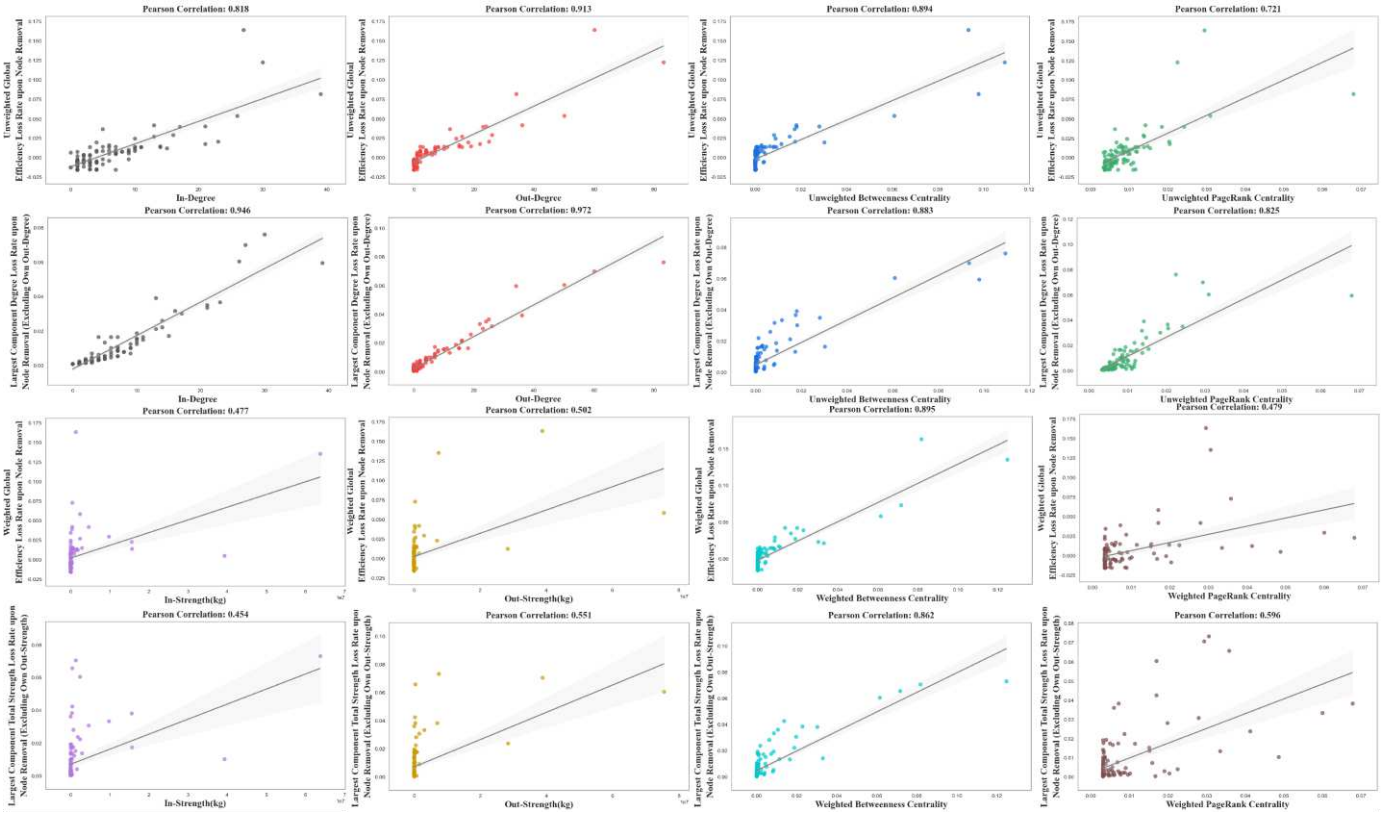


Fig. 12. Correlation between node centrality and network performance loss rate in 2023.

Fig. 12 demonstrates that polysilicon trade network vulnerability diverges markedly between unweighted and weighted dimensions. At the topological level, out-degree strongly correlates with network losses (reaching 0.972), identifying high-connectivity nodes as core pillars. However, in the weighted network, correlations for trade strength and PageRank decline substantially (0.45–0.60), while only weighted betweenness centrality remains robust (above 0.86). This suggests that in a volume-integrated network, node disruptiveness depends on occupying structurally unavoidable bottlenecks within flow pathways rather than mere trade scale. Such irreplaceable hubs, even without peak trade volumes, are essential for preserving global circulation efficiency.

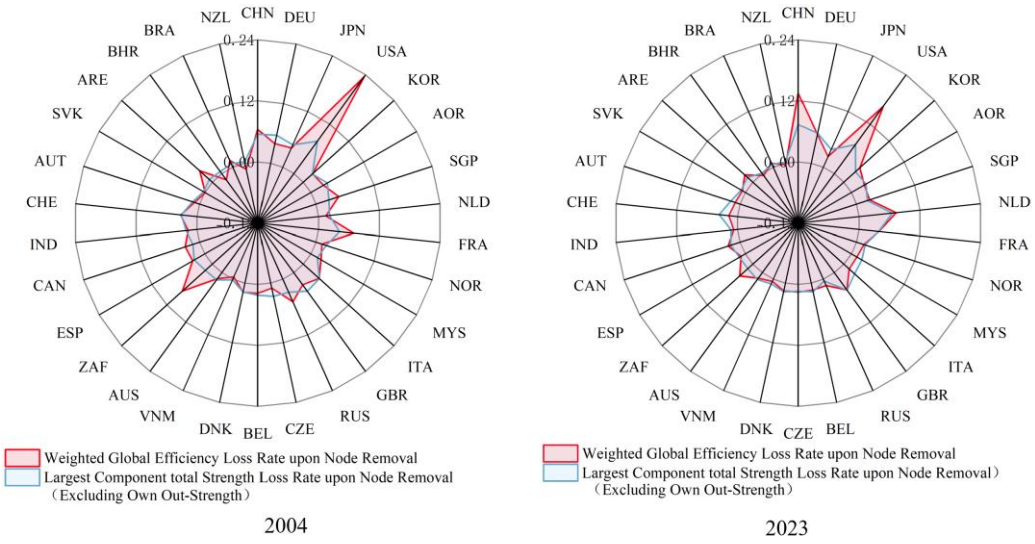


Fig. 13. Radar chart of network performance loss rate after core node disruption in 2004 and 2023.

Fig. 13 shows that core nodes' structural influence strengthened universally during 2004–2023. China, Germany, and the Netherlands saw marked increases in global efficiency loss rates, reflecting enhanced control functions. Conversely, the US transitioned from comprehensive dominance toward supply specialization, maintaining stable local flow disruption despite declining global efficiency impact.

Based on disruption indicators, nodes cluster into three categories: **structural intermediaries** (e.g., China, Netherlands), whose core function is maintaining network connectivity; **dual-impact nodes** (e.g., Germany, US), whose failure simultaneously compromises network strength and transmission pathways; and nodes with limited influence. Notably, "channel controllers" like the Netherlands generate substantial efficiency losses despite modest trade volumes. This reveals that network vulnerability extends beyond resource origins to critical intermediaries; their failure can precipitate systemic paralysis even amid global capacity sufficiency.

3.3. Evolution of node resilience

To assess node resilience within the global polysilicon trade network, we simulate systemic risk through sequential failure of critical trade hubs. Employing four node removal strategies—random disruption (averaged across 100 iterations), out-strength prioritization, weighted betweenness centrality prioritization, and weighted PageRank centrality prioritization—we progressively eliminate nodes and track decay trajectories of in-strength retention rates for core importing nations, thereby identifying nodes with diminished resilience. Utilizing 2023 trade data and a constant time step Δt as the simulation interval, **Fig. 14** illustrates in-strength retention rate dynamics for core importing nodes under alternative disruption strategies. The simulation duration is set to 50 periods, a threshold ensuring that in-strength retention rates approach zero for most nodes under targeted disruption strategies.

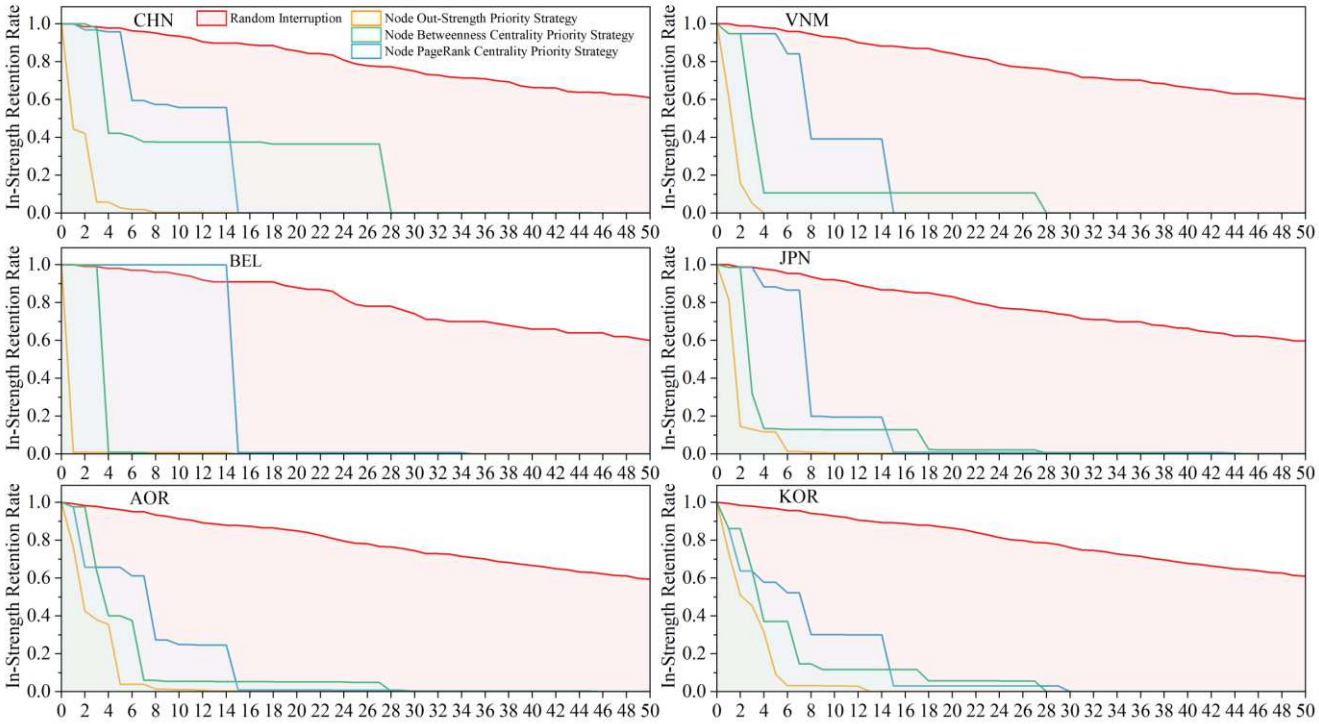


Fig. 14. In-strength retention rate curves of core import nodes under various disruption strategies in 2023.

The simulation results indicate the following. First, disruption strategies yield divergent impacts. Out-strength prioritization, simulating failure of major exporting nations, triggers the most rapid collapse of import capacity. Betweenness centrality disruption, representing failure of critical transshipment hubs, generates heterogeneous effects across countries. PageRank shows intermediate impacts, while random disruption reveals substantial network buffering capacity. This proves that trade network vulnerability stems from both supply concentration and pathway structure. Second, core nations manifest three resilience patterns. Belgium and Vietnam exhibit structural singularity, where capacity collapses abruptly under targeted hits. China demonstrates pathway diversification coupled with supply fragility, showing resilience to transshipment disruptions but extreme sensitivity to exporter loss. Japan and South Korea manifest strategic sensitivity, characterized by rapid initial decline followed by attenuated degradation due to secondary channels.

To elucidate how geopolitical relationships moderate shock transmission, we adopt out-strength prioritization as the baseline attack strategy. By mapping the geopolitical relationship index onto heterogeneous disruption intervals in Eq.(27), we incorporate geopolitical differentiation into the most threatening paths. To magnify initial disparities attributable to varying geopolitical time intervals, **Fig. 15.** In-strength retention rate curves for varying geopolitical time intervals in 2023. compares in-strength retention rates during the first six simulation units, highlighting early-stage dynamic differences under the most disruptive shocks.

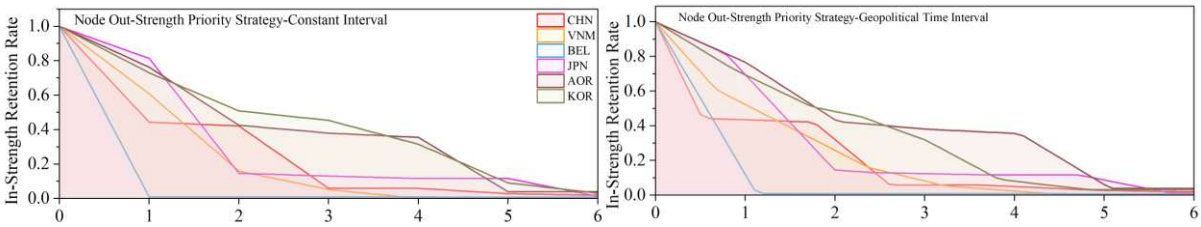


Fig. 15. In-strength retention rate curves for varying geopolitical time intervals in 2023.

The results indicate that, under geopolitical influence, retention rates decline more precipitously for China and South Korea, whereas Vietnam and other Asian regions exhibit trajectories more closely approximating baseline scenarios. This demonstrates that geopolitical relationship indices derived from objective news data effectively quantify and predict node-specific risk exposure within the global polysilicon trade network.

To comparatively analyze shock resistance of core importing nodes under both scenarios, we calculate node resilience following Eqs (26) and (28) (**Fig. 16**). The simulation duration is set to 20 periods, at which point in-strength for all simulated nodes approaches zero.

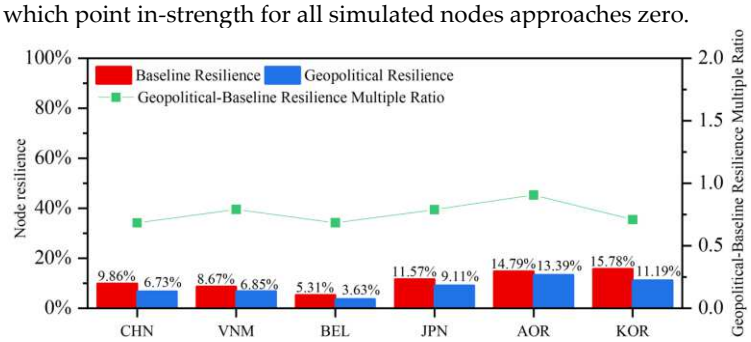


Fig. 16. Comparison of baseline resilience and geopolitical resilience of core import nodes.

Evidently, baseline resilience is directly determined by underlying trade network structure. The rankings clearly reflect this pattern: South Korea and other Asian regions occupy the top two positions, suggesting supply chains characterized by more evenly distributed pathways or dispersed nodes capable of uniformly absorbing shocks; Japan, China, and Vietnam follow, indicating potential network bottlenecks; whereas Belgium ranks lowest, implying excessive dependence on a few critical nodes and structural vulnerability.

When geopolitical risk becomes the disruptive variable, the ranking shifts: other Asian regions ascend to first place, demonstrating successful avoidance of high-risk partners in supply chain architecture; South Korea declines to second, yet maintains high absolute resilience values, exhibiting stability derived from the combination of robust "physical skeleton" and prudent strategic selection. Belgium remains last, exposing dual fragility in both structure and strategy.

To further elucidate long-term evolutionary trends in polysilicon node resilience and the persistent effects of mitigation strategies, **Fig. 17** presents resilience trajectories for six core importing nations under two disruption scenarios during 2004–2023.

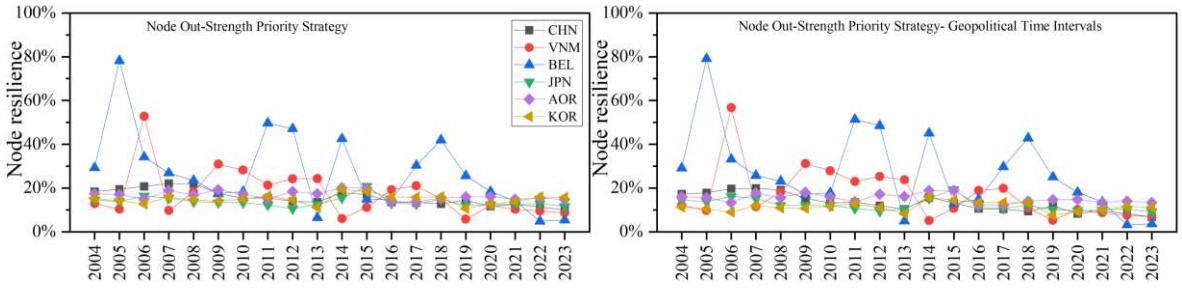


Fig. 17. Evolution of baseline resilience and geopolitical resilience of core import nodes.

Fig. 17 demonstrates that while geopolitically adjusted resilience aligns with the overarching baseline trends, it manifests pronounced heterogeneity in regulatory intensity and perturbation depth. Network topology defines the fundamental "corridor" for resilience evolution, yet geopolitical linkages act as differential modulators. Specifically, China and South Korea undergo consistent resilience suppression due to persistent geopolitical friction, whereas Vietnam and Belgium experience amplified volatility, reflecting a higher sensitivity to bilateral relationship shocks. This suggests that geopolitical risk does not function as a uniform external pressure, but rather as a

node-specific filter that reshapes individual resilience trajectories within the constraints of global trade structure.

4.Conclusions

This study examines the global polysilicon trade network, constructing a complex network model weighted by comprehensive trade distance. We systematically characterize the evolutionary features of trade patterns, structural shifts in node influence, and node resilience under supply disruption shocks during 2004–2023. The main findings are as follows:

(1) Regionalized agglomeration in "supply–processing–demand" trade patterns. Global polysilicon trade has evolved into a regionalized structure with Germany and the U.S. as dual supply hubs, and China and Vietnam as primary processing and demand centers. This high supply-side concentration is driven by both resource endowments and technological barriers.

(2) Functional stratification of node influence. Germany and the U.S. dominate the supply layer through upstream resource and technological control. In contrast, China and Vietnam, despite substantial trade volumes, function as high-import-dependent "processing and demand hubs" rather than core nodes in the supply dimension.

(3) Escalating supply-side fragility amid network efficiency gains. Strengthened trade linkages have enhanced weighted global efficiency; however, deepening negative assortativity and hierarchy indicate that trade intensity is further concentrating within a few supplier nations. While optimizing efficiency, this structure significantly amplifies network sensitivity to supply-side disruptions.

(4) Topological determination of resilience with geopolitically differentiated modulation. Node resilience is fundamentally defined by the "evolutionary corridor" of the network topology, while geopolitical linkages act as differential modulators. Geopolitical risk does not function as a uniform external pressure but as a node-specific filter that exerts asymmetric correction and perturbation on individual resilience trajectories through bilateral linkages.

The key innovations of this study include:

(1) Integrated framework for geopolitical-resilience assessment. We developed a politically sensitive resilience model by mapping a GDELT-based geopolitical relationship index onto heterogeneous disruption intervals. This transcends the conventional homogeneous shock assumption, enabling contextualized simulation of risk transmission where geopolitical linkages act as differential modulators within the topological "evolutionary corridor."

(2) Comprehensive trade distance-weighted network modeling. By synthesizing trade intensity, export competition, and geopolitical relationships, we constructed a dual-weight directed network capturing both "trade flow" and "trade resistance." This approach significantly enhances the structural resolution and realistic explanatory power of strategic intermediate goods trade representations.

(3) Systematic revelation of polysilicon trade evolution. This study provides the first long-term characterization of trade patterns, node influence, and resilience for polysilicon. It demonstrates that geopolitical risk functions as a node-specific filter, exerting asymmetric perturbations on individual resilience trajectories within the constraints of global trade structure.

Policymakers should transition from pure efficiency-seeking to a resilience-oriented framework by diversifying supply sources and strengthening regional collaboration. Crucially, geopolitical risk assessment must be integrated into strategic frameworks to manage the asymmetric shocks identified by our "node-specific filter" mechanism. While providing a robust analytical paradigm, this study remains subject to variations in international trade statistical standards and the news-based nature of the geopolitical index. Future research may extend this framework to other critical minerals or integrate multi-scenario industrial policy simulations to further optimize supply chain risk management.

References

[1] Wang L, Qiu T, Zhang M, Cao Q, Qin W, Wang S, et al. Carbon emissions and reduction performance of photovoltaic systems in China. Renewable and Sustainable Energy Reviews. 2024;200:114603.

[2] Xiang F. Topological analysis, endogenous mechanisms, and supply risk propagation in the polycrystalline silicon trade dependency network. J CLEAN PROD. 2024;439:140657.

[3] Chang NL, Dehghanimadvar M, Egan R. The cost of risk mitigation—Diversifying the global solar PV supply chain. Joule. 2022;6(12):2686-8.

[4] Zhang X, Bai S, Goh M, Guo Y. Climate and geopolitical risk correlations and response decisions for semiconductor global supply chains. Computers & Industrial Engineering. 2024;194:110358.

[5] Li W, Zhang M, Han M. Geographical linkage and trade disruption within global photovoltaic supply chains. Geography and Sustainability. 2025;6(5):100323.

[6] Zhang L, Wang C. Topological Analysis and Robustness Assessment of the Global Polysilicon Trade Network: Implications for Information Management. Conference Topological Analysis and Robustness Assessment of the Global Polysilicon Trade Network: Implications for Information Management. p. 213-22.

[7] Sun S. Research on the Application of Network Analysis Methods in Macroeconomics. Science, Technology and Social Development Proceedings Series. 2024;1:10.70088.

[8] Wang C, Zhang L, Hu X, Zhao Q. Assessing the dynamics of supply risks in the global polysilicon trade network: A multidimensional analysis from 2000 to 2022. Structural Change and Economic Dynamics. 2025;74:991-1007.

[9] Ocaña MG, Al-Moslmi T, Opdahl AL. Knowledge graph semantic annotation and population with real-time events data from GDELT. Conference Knowledge graph semantic annotation and population with real-time events data from GDELT, vol. 2. IEEE, p. 65-72.

[10] Sada S, Oikawa K, Iwasaki F, Ikeda Y. International cooperation analysis of Asian political distance network constructed using event data. Frontiers in Physics. 2022;10:1007796.

[11] Yao Y, Zhang Y, Liu J, Li Y, Li X. Analysis of Spatiotemporal Characteristics and Influencing Factors for the Aid Events of COVID-19 Based on GDELT. Sustainability. 2022;14(19):12522.

[12] Guo Y, Bai R, Hong T. Transboundary cooperation in Arctic climate change governance under geopolitical tensions. J ENVIRON MANAG. 2024;358:120855.

[13] Mo X-M, Yu D-G. Analysis of interaction patterns of intercountry cooperation and conflict events based on complex networks. Conference Analysis of interaction patterns of intercountry cooperation and conflict events based on complex networks. Springer, p. 229-37.

[14] Wang Q, Zhang C, Li R. Impact of different geopolitical factors on the energy transition: The role of geopolitical threats, geopolitical acts, and geopolitical risks. J ENVIRON MANAG. 2024;352:119962.

[15] Liu L, Chen Y, Yu J, Cheng R. Analysis of the trade network of global wood forest products and its evolution from 1995 to 2020. Forest Products Journal. 2024;74(2):121-9.

[16] Fletcher D, Sarkar M. Psychological Resilience: A Review And Critique Of Definitions. Concepts, And Theory, 18 (1), 12–23. 2013.

[17] Hollnagel E, Woods DD, Leveson N. Resilience engineering: Concepts and precepts: Ashgate Publishing, Ltd., 2006.

[18] Huang M, Liu, C., Yu, X., & Jiao, S. Urban water ecological network resilience assessment and optimization strategy: A case study of Changsha City. Economic Geography. 2022;42(10):52-60.

[19] Martin R, Sunley P. On the notion of regional economic resilience: conceptualization and explanation. Journal of economic geography. 2015;15(1):1-42.

[20] Parsons T. The present status of “structural-functional” theory in sociology. The idea of social structure:

Routledge; 2017. p. 67-84.
[21] Wan C, Yang Z, Zhang D, Yan X, Fan S. Resilience in transportation systems: a systematic review and future directions. Transport reviews. 2018;38(4):479-98.
[22] Shao L, Kou W, Zhang H. The evolution of the global cobalt and lithium trade pattern and the impacts of the low-cobalt technology of lithium batteries based on multiplex network. Resources Policy. 2022;76:102550.
[23] Alexander DE. Resilience and disaster risk reduction: an etymological journey. Natural hazards and earth system sciences. 2013;13(11):2707-16.
[24] Meng Y, Zhao X, Liu J, Qi Q. Dynamic influence analysis of the important station evolution on the resilience of complex metro network. Sustainability. 2023;15(12):9309.
[25] Wu Z, Cheng S, Xu K, Qian Y. Ecological network resilience evaluation and ecological strategic space identification based on complex network theory: A case study of Nanjing city. ECOL INDIC. 2024;158:111604.
[26] Xiang Q, Yu H, Huang H, Li F, Ju L, Hu W, et al. Assessing the resilience of complex ecological spatial networks using a cascading failure model. J CLEAN PROD. 2024;434:140014.
[27] Xu C, Xu X. A two-stage resilience promotion approach for urban rail transit networks based on topology enhancement and recovery optimization. Physica A: Statistical Mechanics and its Applications. 2024;635:129496.
[28] Huang XY. Dynamic response mechanism and resilience assessment of the global timber supply network under disruptions (Doctoral dissertation) [Doctor]: Zhongnan University of Forestry and Technology, 2025.
[29] Ji G, Zhong H, Nzudie HLF, Wang P, Tian P. The structure, dynamics, and vulnerability of the global food trade network. J CLEAN PROD. 2024;434:140439.
[30] Jiao B. Research on resilience measurement of international energy trade network from the perspective of energy security. Journal of Industrial Technological Economics. 2024;43(05):131-40.
[31] Yuan X, Ge C, Liu Y, Li N, Wang Y. Evolution of global crude oil trade network structure and resilience. Sustainability. 2022;14(23):16059.
[32] Yu Y, Ma, D., & Wang, X. Trade network resilience of products in the whole industrial chain of international iron ore resources. Resources Science. 2022;44(10):2006-21.
[33] Shen X, Guo, H., & Cheng, J. Resilience assessment of key mineral supply chain network nodes under sudden risk: A case study of nickel products. Resources Science. 2022;44(01):85-96.
[34] Tingting L, Liuguo S. Resilience evaluation of industry and supply chains of clean energy metals in China. Resources Science. 2025;47(4):891-906.
[35] Wu K, Qiu Y, Deng J, Feng Z. The resilience of energy trade networks in countries along “The Belt and Road” and the risk resistance capacity of China. English. 2026:139856.
[36] Wang L, Chen W. Resilience and reconfiguration of global wind power trade networks: Insights from an industrial chain perspective. English. 2025:139519.
[37] Wei N, Xie W-J, Zhou W-X. Resilience of international oil trade networks under extreme event shock-recovery simulations. English. 2025;314:134174.
[38] Zhao Y, Gao J, Zou Z. Trade Network Resilience of the Global Photovoltaic Industry Chain. Journal of Uncertain Systems. 2024;17(04):2450011.
[39] Zhang L, Wen S. The influence of global gallium trade network dynamics on price: A complex network and panel regression approach. Resources Policy. 2024;93:105091.
[40] Choramo TT, Abafita J, Gandica Y, Rocha LE. Economic integration of Africa in the 21st century: Complex network and panel regression analysis. arXiv preprint arXiv:241021019. 2024.
[41] Huang X, Wang Z, Pang Y, Tian W, Zhang M. Static resilience evolution of the global wood forest products trade network: A complex directed weighted network analysis. Forests. 2024;15(9):1665.

[42] Tang B, Wang C, Wu Y, Zhang J, Zou Y. Global Energy Transition under Dynamic Trade Networks: Integrating Complex-Network and Deep Learning Methods. English. 2026:140305.
[43] Wang C, Zhang X, Hu X, Sun B, Zhao L, Lim MK, et al. Evolution of structural characteristics and its determinants of global human hair waste trade network based on temporal exponential random graph model. Resources, Conservation and Recycling. 2024;200:107305.
[44] Shao L, Li, Y., & Lan, T. Research on the synergistic development path of gallium resources sustainable supply and China aluminum emission reduction under the associated mechanism. Journal of Central South University (Social Science). 2025;31(03):138-53.
[45] Project G. Global Database of Events, Language, and Tone (GDELT). 2013.
[46] Buckingham K, Brandt J, Anderson W, do Amaral LF, Singh R. The untapped potential of mining news media events for understanding environmental change. Current Opinion in Environmental Sustainability. 2020;45:92-9.
[47] Hong D, Fu Z, Zhang X, Pan Y. Research on the Development and Application of the GDELT Event Database. Data. 2025;10(10):158.
[48] Suhua O, Jian L, Qingshan Y. Evolution of the Global Semiconductor Trade Dependence Networks and Its Risk Relationship Identification: Concurrent Discussion on the Change of China's Status. Economic geography. 2024;44(12):101-12.
[49] Zheng Y, Lucey B. What REALLY drives clean energy stocks-Fear or Fundamentals? Energy Economics. 2025;148:108558.
[50] Li Y, Ding Y, Guo Y, Cui H, Gao H, Zhou Z, et al. An integrated decision model with reliability to support transport safety system analysis. RELIAB ENG SYST SAF. 2023;239:109540.
[51] Tian W, Huang X, Shao L, Wang Z, Li Y. Assessment and evolution analysis of the global wood pulp trade network resilience based on underload cascading failure. J CLEAN PROD. 2025;518:145742.
[52] Huang X, Wang Z, Pang Y, Tian W. Evolution of disruption resilience in the wood forest products trade network, considering the propagation of disruption risks and underload cascading failure. Sustainability. 2025;17(6):2733.
[53] Germann J. Global rivalries, corporate interests and Germany's 'National Industrial Strategy 2030'. Review of international political economy. 2023;30(5):1749-75.
[54] Zhang Y, Zhu X. Analysis of the global trade network of the chip industry chain: Does the US-China tech war matter? Heliyon. 2023;9(6).
[55] Woods N. The globalizers: the IMF, the World Bank, and their borrowers: Cornell University Press, 2006.
[56] Hughes L, Meckling J. The politics of renewable energy trade: The US-China solar dispute. Energy Policy. 2017;105:256-62.
[57] Abdelilah Y, Bahar H, Briens F, Bojek P, Criswell T, Kurumi K, et al. Special report on solar PV global supply chains. Tech rep, International Energy Agency. 2022.
[58] Basore P, Feldman D. Solar photovoltaics: Supply chain deep dive assessment. USDOE Office of Policy (PO), Washington DC (United States); Oak Ridge …; 2022.